Hydrol. Earth Syst. Sci., 18, 3499–3509, 2014
www.hydrol-earth-syst-sci.net/18/3499/2014/
doi:10.5194/hess-18-3499-2014

Hydrology and Earth System Sciences
Open Access

Attribution of satellite-observed vegetation trends in a hyper-arid region of the Heihe River basin, Western China

Y. Wang[1,2,3,4], **M. L. Roderick**[4,5,6], **Y. Shen**[1], **and F. Sun**[4,6]

[1]Key Laboratory of Agricultural Water Resources, Hebei Key Laboratory of Agricultural Water-Saving, Center for Agricultural Resources Research, Institute of Genetics and Developmental Biology, Chinese Academy of Sciences, Shijiazhuang, 050021, China
[2]University of Chinese Academy of Sciences, Beijing, 10049, China
[3]Research Center for Hebei Ecological Environmental Construction, Hebei Academy of Social Sciences, Shijiazhuang, 050051, China
[4]Research School of Biology, The Australian National University, Canberra, 0200, Australia
[5]Research School of Earth Science, The Australian National University, Canberra, 0200, Australia
[6]Australian Research Council Centre of Excellence for Climate System Science, Canberra, Australia

Correspondence to: Y. Shen (yjshen@sjziam.ac.cn)

Received: 8 December 2013 – Published in Hydrol. Earth Syst. Sci. Discuss.: 5 February 2014
Revised: 17 June 2014 – Accepted: 30 July 2014 – Published: 9 September 2014

Abstract. Terrestrial vegetation dynamics are closely influenced by both climate and by both climate and by land use and/or land cover change (LULCC) caused by human activities. Both can change over time in a monotonic way and it can be difficult to separate the effects of climate change from LULCC on vegetation. Here we attempt to attribute trends in the fractional green vegetation cover to climate variability and to human activity in Ejina Region, a hyper-arid landlocked region in northwest China. This region is dominated by extensive deserts with relatively small areas of irrigation located along the major water courses as is typical throughout much of Central Asia. Variations of fractional vegetation cover from 2000 to 2012 were determined using Moderate Resolution Imaging Spectroradiometer (MODIS) vegetation index data with 250 m spatial resolution over 16-day intervals. We found that the fractional vegetation cover in this hyper-arid region is very low but that the mean growing season vegetation cover has increased from 3.4 % in 2000 to 4.5 % in 2012. The largest contribution to the overall greening was due to changes in green vegetation cover of the extensive desert areas with a smaller contribution due to changes in the area of irrigated land. Comprehensive analysis with different precipitation data sources found that the greening of the desert was associated with increases in regional precipitation. We further report that the area of land irrigated each year can be predicted using the runoff gauged 1 year earlier. Taken together, water availability both from precipitation in the desert and runoff inflow for the irrigation agricultural lands can explain at least 52 % of the total variance in regional vegetation cover from 2000 to 2010. The results demonstrate that it is possible to separate the satellite-observed changes in green vegetation cover into components due to climate and human modifications. Such results inform management on the implications for water allocation between oases in the middle and lower reaches and for water management in the Ejina oasis.

1 Introduction

Terrestrial vegetation plays a key role in energy, water, and biogeochemical cycles, and changes in vegetation can also significantly influence atmospheric processes (Pielke et al., 1998; Gerten et al., 2004). Monitoring of terrestrial vegetation dynamics therefore underpins efforts to better understand the feedbacks between vegetation and the atmosphere (Bonan et al., 2003; Bounoua et al., 2010; Angelini et al., 2011). In particular, the Normalized Difference Vegetation Index (NDVI) derived from satellite observations of red and near-infrared reflectance has proven useful in assessing

vegetation dynamics from regional to global scales (Tucker, 1979; Box et al., 1989; Fensholt et al., 2013).

Greening trends have been detected on global (Myneni et al., 1997; Nemani et al., 2003; Donohue et al., 2013; Fensholt et al., 2013) and regional (Fang et al., 2004; Herrmann et al., 2005; Donohue et al., 2009) scales, but attribution of those trends in terms of the underlying biophysical and socioeconomic causes remains a difficult task. The central challenge is that vegetation can change for a myriad of reasons including changes in the local climate (e.g., rainfall, radiation, temperature, humidity.) (Myneni et al., 1997; Goetz et al., 2005; Donohue et al., 2009), biogeochemistry (e.g., atmospheric CO_2, nutrient deposition.) (Lim et al., 2004; Bond et al., 2003; Donohue et al., 2013; Dirnböck et al., 2014), ecological processes (e.g. long-term successional recovery from disturbance, fire dynamics, disease.) (Thonicke et al., 2001; Bond et al., 2003), and via direct anthropogenic activity (e.g., land use change, irrigation, agriculture) (Hutchinson et al., 2000; Thonicke et al., 2001). One approach to handle this complexity is to use regional knowledge to constrain the problem.

In terms of the attribution of regional vegetation trends, the landscapes typical of Central Asia present a unique challenge. The region is hyper-arid with annual precipitation in many areas of often less than 50 mm, with hot summers and cold winters. What is of particular interest throughout Central Asia is the presence of many localized regions of irrigated agriculture that often support relatively large local populations. Those irrigation communities are usually located at oases that receive an annual input of water in the form of runoff from surrounding mountains. Much of the outflow from the mountains is recent precipitation (snowmelt) but a further complication of recent years is that glacier melt has augmented the snowmelt and increased inflow of water to many oases throughout Central Asia (Yao et al., 2004; Lioubimtseva and Henebry, 2009; Rahimov, 2009; Unger-Shayesteh et al., 2013). Time series of NDVI satellite imagery generally show greening trends over Central Asia (Fang et al., 2004; Mohammat et al., 2013). However, in terms of overall water resources management it is important to understand what caused the overall greening (or browning) trend. For example, did it arise because of an expansion (or contraction) of the area being irrigated? Or alternatively, the irrigated area might have remained more or less constant and any large-scale greening (or browning) trend in vegetation might be related to subtle yet detectable changes in vegetation cover in the extensive deserts of Central Asia. The management implications are quite different for those two scenarios and require a clear separation of these sources of variation.

In this paper, we investigate satellite-observed (MODIS) vegetation trends (NDVI) in a hyper-arid region of the Heihe River basin located in northwest China. The aim of this study is to test whether it is possible to separate the vegetation trends in a small relatively well-studied basin into components due to climate and due to changes in irrigation. We believe that the method may be widely applicable throughout Central Asia.

2 Data and methods

2.1 Study area

We examined part of the landlocked Heihe River basin in northwest China (40°20′–42°40′ N, 97°30′–101°45′ E) (Fig. 1). Our study area occupies the downstream (northern) part of the basin (Fig. 1b) and is serviced by the regional center, Ejina, which currently has a population of around 30 000 (http://www.geohive.com/cntry/cn-15.aspx). The hydroclimate of this predominantly desert environment is extreme. As an indication, at Ejina, the mean annual temperature is around 8 °C but daytime excursions in the summer reach 42 °C while nighttime temperatures drop to −36 °C during winter (Y. C. Zhang et al., 2011). The mean annual precipitation over the extensive flatlands is typically less than 50 mm (Fig. 1a) while the mean annual pan evaporation is typically around 3500 mm (Jin et al., 2010; Jia et al., 2011; Wang et al., 2013b). Agriculture is only possible via irrigation that is located immediately adjacent to the Heihe River (Fig. 1c). The study area ($\sim 80\,000\,km^2$) is located within the broader Gobi Desert and also hosts the second largest area of *Populus euphratica* and *Haloxylon ammodendron* forests in China. The basin is generally considered to be the main ecobarrier in northern China (Fu et al., 2007; Qin et al., 2012).

The Heihe River (Fig. 1b) is the second longest inland river in China and is the sole river flowing through the Ejina Region (Guo et al., 2009). This river originates in the Qilian Mountains. After reaching the mountain outlet at the Yingluoxia hydrological gauge station (Fig. 1b), it flows through several oases (Zhangye, Gaotai, Dingxin, Ejina) before terminating at the East and West Juyan lakes. Zhengyixia station is located downstream of those main oases, where most water is consumed for agriculture. The discharge at Zhengyixia typically peaks around September each year while the growing season extends from April to October (Fig. 2a). Consequently, the irrigated crops in the northern parts of the basin use irrigation water that was discharged from the mountains some 6 months earlier.

The river discharge from the mountain regions has shown an increasing trend in past decades. Annual discharge observed at Yingluoxia site increased to $15.7 \times 10^8\,m^3$ in the 1990s from around $14.4 \times 10^8\,m^3$ in the 1960s (Fig. 2b). However, the discharge observed at Zhengyixia station located at the place after the river flowing through the oases decreased from around $10.5 \times 10^8\,m^3$ in the 1960s to around $7.5 \times 10^8\,m^3$ in the 1990s. The increasing water withdrawal in the upper and middle reaches since the 1960s was associated with increased irrigation (and associated industrial development and urbanization) that made significant reductions

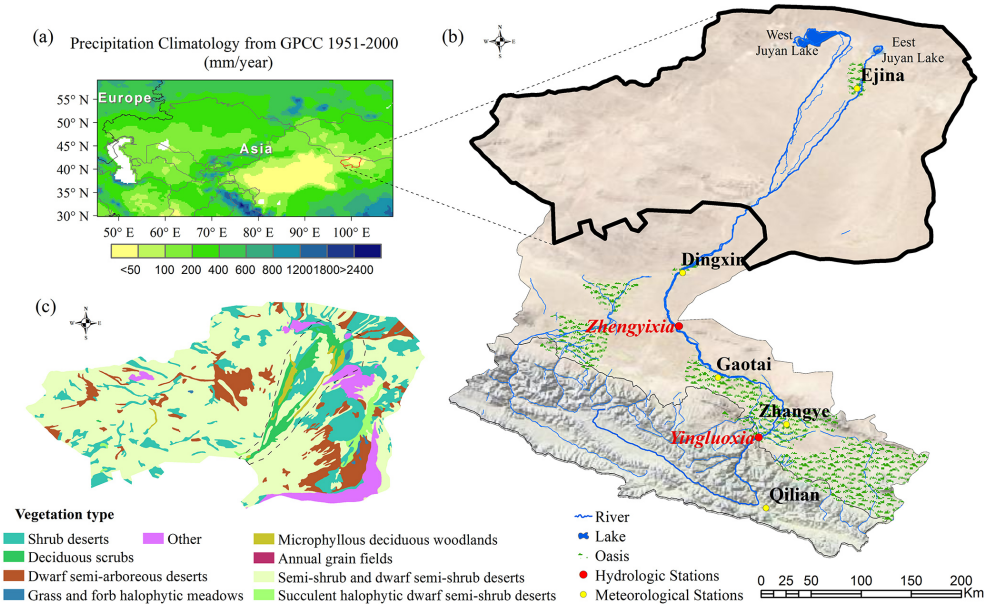

Figure 1. Details of the study area. Regional setting and the mean annual precipitation (1951–2000) **(a)**. Landscape of Heihe River basin with location of meteorological and hydrologic observation sites **(b)**. Vegetation map of lower Heihe River basin where the dashed line denotes the bounds of the possible irrigation area **(c)**.

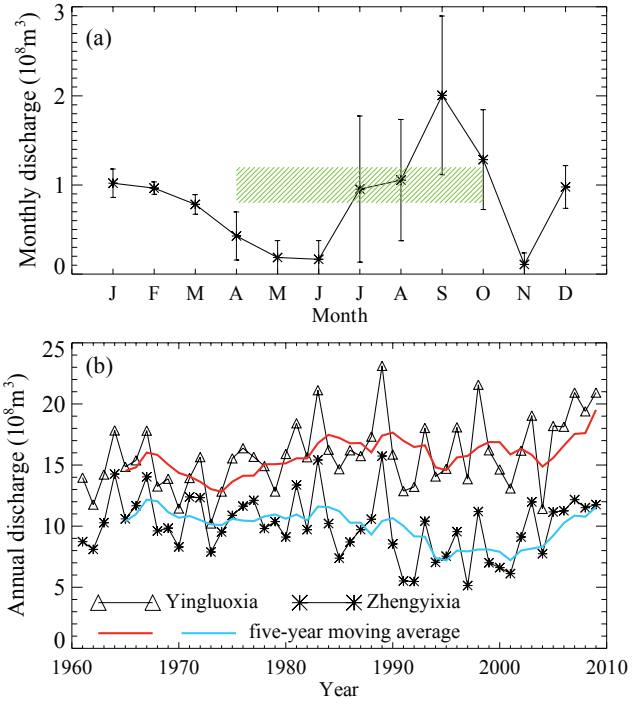

Figure 2. River flows in the Heihe River basin. Mean monthly river discharge (bars indicate standard deviation) of Heihe River (2000–2009) at Zhengyixia station in relation to the growing season (diagonal stripes) **(a)**. Annual discharge of Heihe River (1961–2009) at Yingluoxia and Zhengyixia stations **(b)**.

in river flows to the downstream oases and accelerated desertification in the northern parts of the basin (Guo et al., 2009; Jin et al., 2010). This phenomenon resulted in the drying up of East Juyan Lake in 1992 and the drying up of West Juyan Lake even earlier (Guo et al., 2009).

To restore the ecosystem of the downstream Heihe River basin the Ecological Water Conveyance Project (EWCP) was launched by the Chinese government. Water use has been regulated (reduced) since around the year 2000 in the middle parts of the basin, thereby delivering more water to the terminal lakes in the northern extremities of the basin (Y. C. Zhang et al., 2011). In the past decade (2000–2009) the average flow at Zhengyixia has increased to levels (about 10.5×10^8 m^3) not seen since the 1960s (Y. C. Zhang et al., 2011; Qin et al., 2012). One aim was to reduce degradation of the ecological environment in the northern extremities. Since 2000, an increase in native vegetation growth and species diversity has been attributed to increased groundwater recharge from the increased flows making their way into the northern parts of the basin (Jin et al., 2010; Jia et al., 2011).

In summary, the basin is a classic source–sink system with water sourced (via snowmelt and glacier melt) in the humid mountains in the south that subsequently flows northwards to terminal sinks at the East and West Juyan lakes. With this background, we note that many studies have reported trends in vegetation in particular subregions of the basin (Jin et al., 2010; Jia et al., 2011; Wang et al., 2011) but there has yet to be a comprehensive assessment of vegetation trends in the study area. A basin-wide assessment that is useful for hydrologic management requires separation of the overall

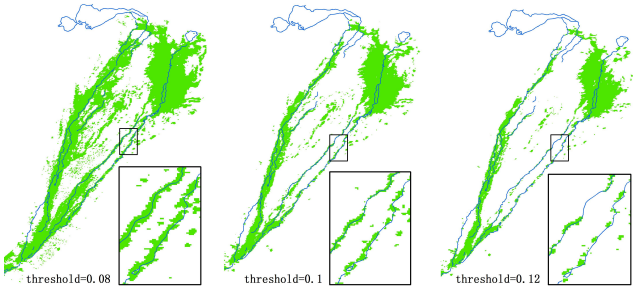

Figure 3. Irrigated areas derived using different NDVI thresholds.

vegetation trend into a component due to irrigation and a component due to changes in the desert vegetation. That is the aim of the current study.

2.2 MODIS satellite observations

Moderate Resolution Imaging Spectroradiometer (MODIS) Terra vegetation indices (MOD13Q1) data were acquired from the National Aeronautics and Space Administration (NASA) Earth Observing System Data and Information System (http://reverb.echo.nasa.gov) with spatial resolution of 250 m and temporal resolution of 16 days between April 2000 and December 2012. We used the Savitzky–Golay filter (Chen et al., 2004) to minimize noise in the NDVI series prior to further processing. Exploratory analysis highlighted anomalously low NDVI values during many of the winter months that coincided with snow/ice cover. To avoid those anomalous values we restricted the time series to cover the 7-month growing season (April–October).

2.3 Identifying the irrigated areas

The irrigation regions of interest are restricted to the immediate vicinity of the Heihe River (within the dashed line in Fig. 1c). Within that zone, irrigation is usually supplied by the extraction of groundwater and it is very difficult to distinguish agricultural vegetation from native vegetation that is drawing upon groundwater reserves in the satellite imagery. From the point of view of water resource management, both vegetation types use the same groundwater resources and we made no distinction between them. That enabled us to use a simple threshold approach to identify the vegetated areas of interest because they have much higher green vegetation cover during the April–October growing season.

To identify the irrigated area we created a composite image for each year (2000–2012) showing the maximum NDVI recorded during the April–October growing period. We first estimated the mean of the maximum NDVI over adjacent desert regions and found an NDVI of 0.0996 (±0.024). On that basis we initially defined the irrigated areas as being within the river zone (Fig. 1c) and having an annual maximum NDVI greater than 0.10. To test that threshold we used field surveys showing that irrigated vegetation (that includes native vegetation accessing groundwater) can exist up to a kilometer from the main east river channel in a central part of the basin since the water conveyance project was launched (Guo et al., 2009). We varied the NDVI threshold (0.08, 0.10, 0.12; see Fig. 3) and visually estimated the lateral extent of the vegetation from the river channel. At a threshold of 0.08, the implied irrigation area extended further than 1 km from the main channel while at a threshold of 0.10 the extent was some 200–1000 m from the river channel and consistent with field surveys (Guo et al., 2009). When the NDVI threshold was set at 0.12, the irrigated area was (incorrectly) shown to be discontinuous (Fig. 3). With that result we were confident that a threshold of 0.10 would correctly identify irrigated areas as defined. That threshold was used to classify the basin land cover into two classes, desert and irrigation, for each year of the period 2000–2012.

2.4 Converting NDVI to fractional vegetation cover

Fractional vegetation cover (f_V) was computed from NDVI (V) using a simple linear scaling (Carlson and Ripley, 1997):

$$f_V = (V - V_{min}) / (V_{max} - V_{min}), \quad (1)$$

where V_{min} and V_{max} represent zero green vegetation cover (i.e., bare soil, $f_V = 0$) and complete vegetation cover ($f_V = 1$), respectively. We assume that there are regions of bare soil (e.g., desert) and of complete vegetation cover (e.g., irrigated agriculture) in the study area of sufficient size relative to the MODIS spatial resolution (250 m) to define the limits of our scaling. To identify those limits we first composited the annual (April–October) maximum V image into a single maximum V image for the entire 13-year (2000–2012) study period. We then conducted a detailed examination of the desert regions and identified an NDVI threshold of 0.05 that was equated to bare ground ($f_V = 0$). To identify the upper limit, we investigated small regions of agricultural crops in the maximum composite and identified an NDVI threshold of 0.65 that was equated to full cover ($f_V = 1$). Those thresholds were used (in Eq. 1) to rescale the NDVI data into fractional vegetation cover with values outside the range set to the respective limits.

2.5 Attribution of vegetation changes

With the region split into two land cover types, the regional fractional vegetation cover (f_V) is determined by fractional vegetation coverage of the irrigated (f_I) and non-irrigated (f_D) areas and the respective areas (A_I, A_D) for each year,

$$f_V = \frac{A_I * f_I + A_D * f_D}{A_I + A_D}. \quad (2a)$$

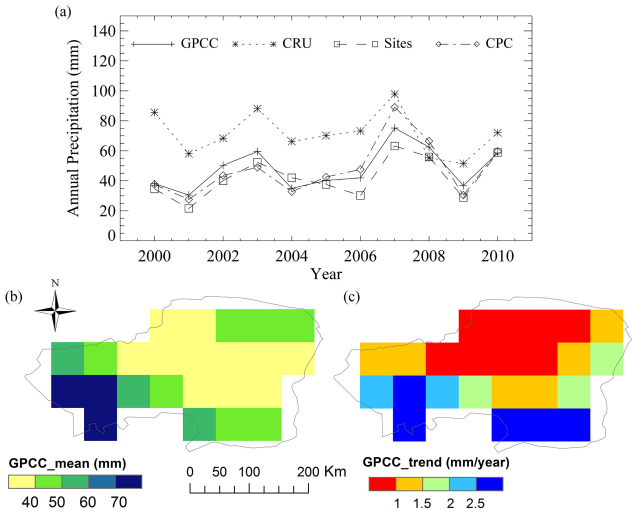

Figure 4. Spatiotemporal change of precipitation for the study area. **(a)** Annual precipitation for four different data sources (as indicated)**(a)**; Mean annual precipitation from GPCC **(b)**, and the trend from 2000 to 2010 **(c)**.

Defining the area fractions $A_{\mathrm{I}}^{*}\left(=\frac{A_{\mathrm{I}}}{A_{\mathrm{I}}+A_{\mathrm{D}}}\right)$ and $A_{\mathrm{D}}^{*}\left(=\frac{A_{\mathrm{D}}}{A_{\mathrm{I}}+A_{\mathrm{D}}}\right)$ with $A_{\mathrm{I}}^{*}+A_{\mathrm{D}}^{*}=1$, we rewrite Eq. (2a) as

$$f_{\mathrm{V}}=A_{\mathrm{I}}^{*}*f_{\mathrm{I}}+A_{\mathrm{D}}^{*}*f_{\mathrm{D}}. \tag{2b}$$

The total differential $\mathrm{d}f_{\mathrm{V}}$ is

$$\begin{aligned}\mathrm{d}f_{\mathrm{V}}&=\frac{\partial f_{\mathrm{V}}}{\partial f_{\mathrm{I}}}\mathrm{d}f_{\mathrm{I}}+\frac{\partial f_{\mathrm{V}}}{\partial A_{\mathrm{I}}^{*}}\mathrm{d}A_{\mathrm{I}}^{*}+\frac{\partial f_{\mathrm{V}}}{\partial f_{\mathrm{D}}}\mathrm{d}f_{\mathrm{D}}+\frac{\partial f_{\mathrm{V}}}{\partial A_{\mathrm{D}}^{*}}\mathrm{d}A_{\mathrm{D}}^{*},\\&=A_{\mathrm{I}}^{*}\,\mathrm{d}f_{\mathrm{I}}+f_{\mathrm{I}}\,\mathrm{d}A_{\mathrm{I}}^{*}+A_{\mathrm{D}}^{*}\,\mathrm{d}f_{\mathrm{D}}+f_{\mathrm{D}}\,\mathrm{d}A_{\mathrm{D}}^{*}.\end{aligned} \tag{3}$$

The relative change in f_{V} is given by

$$\begin{aligned}\frac{\mathrm{d}f_{\mathrm{V}}}{f_{\mathrm{V}}}&=\frac{A_{\mathrm{I}}^{*}f_{\mathrm{I}}}{f_{\mathrm{V}}}\frac{\mathrm{d}f_{\mathrm{I}}}{f_{\mathrm{I}}}+\frac{f_{\mathrm{I}}}{f_{\mathrm{V}}}\mathrm{d}A_{\mathrm{I}}^{*}+\frac{A_{\mathrm{D}}^{*}f_{\mathrm{D}}}{f_{\mathrm{V}}}\frac{\mathrm{d}f_{\mathrm{D}}}{f_{\mathrm{D}}}+\frac{f_{\mathrm{D}}}{f_{\mathrm{V}}}\mathrm{d}A_{\mathrm{D}}^{*}\\&=X_{f_{\mathrm{I}}}+X_{A_{\mathrm{I}}}+X_{f_{\mathrm{D}}}+X_{A_{\mathrm{D}}}.\end{aligned} \tag{4}$$

where the various X terms on the right-hand side denote the total change in f_{V} due to changes in the greenness ($X_{f_{\mathrm{I}}}$, $X_{f_{\mathrm{D}}}$) and fractional area ($X_{A_{\mathrm{I}}}$, $X_{A_{\mathrm{D}}}$).

2.6 Estimates of water availability

The vegetation trends are ultimately compared to estimates of trends in water availability over the desert and in the irrigation area. We used the monthly discharge gauged at Zhengyixia (Fig. 1b) as a measure of the inflow available for irrigation in Ejina. Over the desert parts of the region, precipitation represents the only input of water. To estimate water availability via precipitation we used three gridded databases ($0.5^{\circ}\times 0.5^{\circ}$, monthly, 2000–2010) from the Global Precipitation Climatology Centre (GPCC) (Schneider et al., 2008), Climatic Research Unit (CRU) TS 3.10 (Harris et al., 2013), and the Climate Prediction Center (CPC) (Chen et al., 2002). We also averaged the data from two local meteorological sites (Ejina, Dingxin; see Fig. 1b) as a further check on the gridded databases. Initial analysis showed that precipitation (P) was generally a little higher in the CRU database (but with similar interannual variability) while the other two remaining databases gave similar spatial patterns, variability, and trends (Fig. 4 and Supplement Fig. S1). We were most familiar with the GPCC database following previous work (Sun et al., 2012) and subsequently adopted the GPCC database as the precipitation record for the study area (Fig. 4b, c). Note that final interpretations and our conclusions are not sensitive to the choice of precipitation database and we also present the complete analysis using the other spatial databases (CRU, sites, and CPC) in the Supplement.

3 Results

3.1 Vegetation trends

The fractional vegetation cover f_{V} in this hyper-arid region is very low, with mean growing season f_{V} of about 3–4 %. The oases systems are clearly distinguished by the much higher vegetation cover (Fig. 5a and Supplement Fig. S2). Over the 13-year period (2000–2012) the mean growing season fractional vegetation cover (f_{V}) showed an increase trend overall, especially in the irrigated oasis (Fig. 5b). The annual maximal fractional vegetation cover changed similarly (Fig. S2 in the Supplement). The mean annual fractional vegetation for the whole region increased steadily starting at about 3.2 % in 2000 and rising to around to 4.5 % in 2012 (Fig. 5c).

The mean growing season fractional vegetation cover in the extensive desert regions (f_{D}) more or less tracked the changes in the regional total (f_{V}). The area classified as irrigated only occupies around 3 % of total study area with a relatively high growing season average vegetation cover f_{I} of around 17%. Over the 2000–2012 period, the fractional irrigation area (A_{I}^{*}) showed a steady increase (from 3 to 4 %) and the mean growing season fractional vegetation cover (f_{I}) also increased from around 16 to 18 %.

3.2 Sensitivity analysis and trend attribution

3.2.1 Sensitivity

After substituting the relevant numerical values ($f_{\mathrm{V}}=0.039$, $f_{\mathrm{I}}=0.174$, $A_{\mathrm{I}}^{*}=0.033$, $f_{\mathrm{D}}=0.035$, $A_{\mathrm{D}}^{*}=0.967$) derived from the mean growing season (2000–2012) into Eq. (4), the relative change in f_{V} is

$$\frac{\mathrm{d}f_{\mathrm{V}}}{f_{\mathrm{V}}}=0.15\frac{\mathrm{d}f_{\mathrm{I}}}{f_{\mathrm{I}}}+4.45\mathrm{d}A_{\mathrm{I}}^{*}+0.85\frac{\mathrm{d}f_{\mathrm{D}}}{f_{\mathrm{D}}}+0.88\mathrm{d}A_{\mathrm{D}}^{*}. \tag{5}$$

The coefficients in Eq. (5) denote the different sensitivities to change in the overall regional vegetation cover. From that

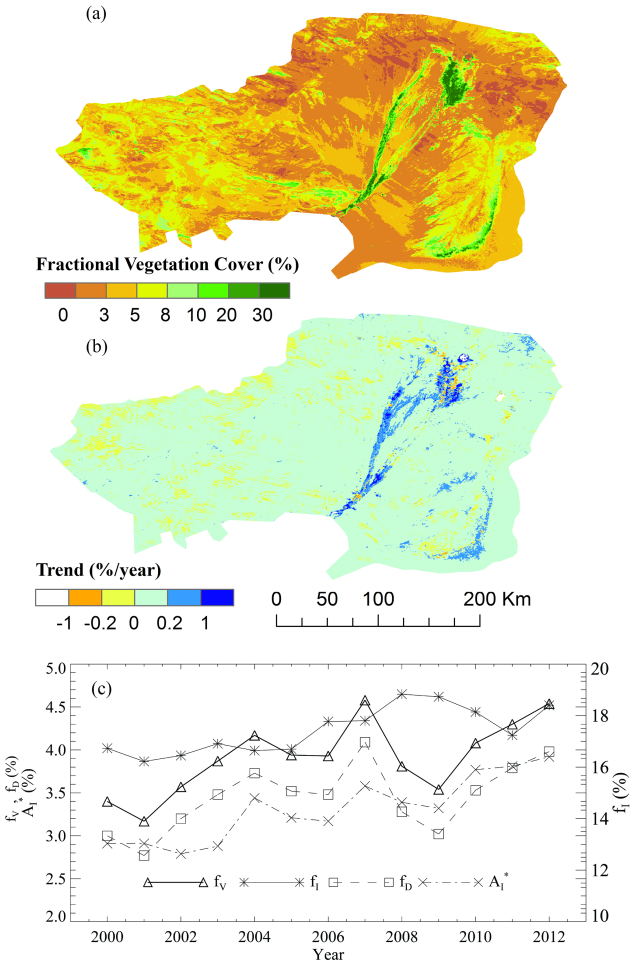

Figure 5. Spatiotemporal change of the growing season (April–October) mean annual fractional vegetation cover (2000–2012). Spatial pattern of growing season (April–October) mean annual fractional vegetation cover **(a)**; spatial trend of growing season (April–October) mean annual fractional vegetation cover (2000–2012) **(b)**; trends in the growing season (April–October) mean annual fractional vegetation for the whole region (f_V, left axis), desert (f_D, left axis), and irrigated (f_I, right axis) land cover classes, and for the fractional area of irrigation (A_I^*, left axis) **(c)**.

equation we infer that the relative change in fractional green vegetation is most sensitive to variations in the fractional irrigation area (A_I^*). Note that regional vegetation cover is also a factor of around 6 (0.85/0.15) times more sensitive to variations in greenness over the desert than over the irrigated regions because the desert land-cover type dominates the total area.

3.2.2 Trend attribution

From 2000 to 2012, the regional f_V increased by $\sim 25\,\%$. In terms of the underlying components, the causes of those changes varied from year to year (Fig. 6) but the largest contribution was generally due to changes in f_D (see X_{f_D} in Fig. 6) with a smaller contribution due to changes in A_I^* (X_{A_I} in Fig. 6). Variations in the remaining terms (X_{f_I}, X_{A_D}) had little impact on trends in the overall regional vegetation cover.

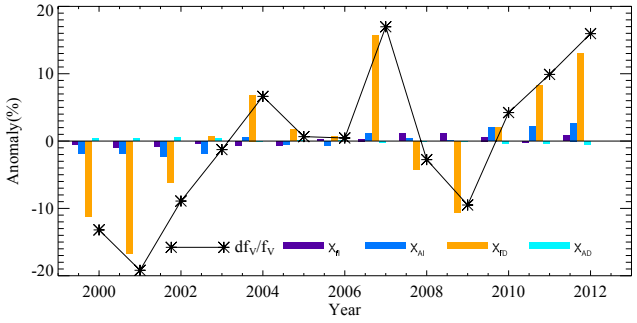

Figure 6. Annual changes in relative vegetation cover ($\mathrm{d}f_V/f_V$) and the underlying components from mean annual fractional vegetation for the desert (X_{f_D}) and for the irrigated (X_{f_I}) regions along with changes due to changes in the fractional area of desert (X_{A_D}) and irrigated (X_{A_I}), regions.

3.2.3 Uncertainty analysis

The major source of uncertainty in our results relates to the NDVI threshold used to distinguish the irrigated and desert regions (Sect. 2.3, Fig. 3). To evaluate the robustness of our results we also calculated the relative change in fractional vegetation cover using five different NDVI thresholds (0.08, 0.09, 0.10, 0.11, 0.12; Table 1). Those results show that while the numerical value of the sensitivity coefficients does change, the overall conclusion that regional vegetation cover is most sensitive to changes in irrigation area remains unchanged. Similarly, the attribution results for different thresholds show that most of the change in regional vegetation cover remained due to changes in desert greenness and in the area of irrigation.

3.3 Predicting regional vegetation cover based on water availability

The earlier results (Sects. 3.2.2, 3.2.3) show that the regional vegetation cover trend mainly depends on fractional vegetation cover over the extensive desert regions and the area of the irrigated lands. With that result, we approximate Eq. (4) as

$$\frac{\mathrm{d}f_V}{f_V} \sim \frac{f_I}{f_V}\mathrm{d}A_I^* + \frac{A_D^*}{f_V}\mathrm{d}f_D. \quad (6)$$

In this region, the area of land irrigated each year is dependent on the inflow at an earlier time while greenness in the desert areas is dependent on precipitation. To test this, we use the 12-month GPCC precipitation estimate to the end of the growing season (the previous November–October) to estimate the growing season desert vegetation cover. The results

Table 1. Sensitivity and attribution uncertainty with varied NDVI thresholds to define irrigated and non-irrigated regions (mean annual fractional vegetation for the whole region f_V, irrigated oasis f_I and desert f_D, fractional area of irrigation A_I^* and desert A_D^*, and their attribution X_{f_I}, X_{A_I}, X_{f_D}, X_{A_D}).

NDVI Threshold	Sensitivity	Attribution			
		X_{f_I}	X_{A_I}	X_{f_D}	X_{A_D}
0.08	$\frac{df_V}{f_V} = 0.18\frac{df_I}{f_I} + 2.97 dA_I^* + 0.82\frac{df_D}{f_D} + 0.88 dA_D^*$	14.0 %	16.8 %	74.1 %	−5.0 %
0.09	$\frac{df_V}{f_V} = 0.16\frac{df_I}{f_I} + 3.76 dA_I^* + 0.84\frac{df_D}{f_D} + 0.88 dA_D^*$	9.5%	19.4%	75.6%	−4.5%
0.1	$\frac{df_V}{f_V} = 0.15\frac{df_I}{f_I} + 4.45 dA_I^* + 0.85\frac{df_D}{f_D} + 0.88 dA_D^*$	7.8%	20.5%	75.8%	−4.1%
0.11	$\frac{df_V}{f_V} = 0.14\frac{df_I}{f_I} + 4.99 dA_I^* + 0.86\frac{df_D}{f_D} + 0.89 dA_D^*$	7.6%	20.3%	75.7%	−3.6%
0.12	$\frac{df_V}{f_V} = 0.13\frac{df_I}{f_I} + 5.42 dA_I^* + 0.87\frac{df_D}{f_D} + 0.89 dA_D^*$	7.3%	19.4%	76.4%	−3.2%

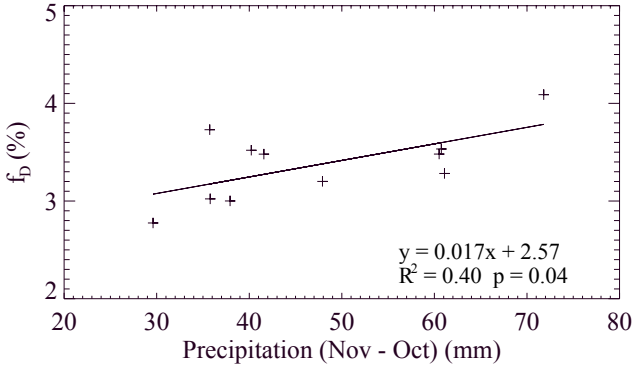

Figure 7. Relationship between growing season desert vegetation cover (f_D) and annual precipitation (per GPCC database 2000–2010).

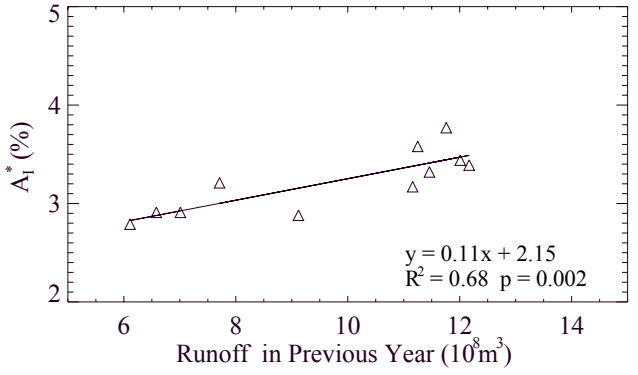

Figure 8. Relationship between fractional irrigated area A_I^* and runoff at Zhengyixia from the previous year 2000–2010.

show a positive relationship ($p < 0.05$, Fig. 7) and imply that the desert vegetation cover increases by 0.017 % for each additional mm of annual P. The analysis based on other precipitation databases (CRU, sites, and CPC) is included in the supporting materials (Fig. S3 and Table S1 both in the Supplement).

We sought a similar predictive relationship between the total runoff (R) in the previous calendar year at Zhengyixia and the fractional irrigated area (A_I^*) (Fig. 8). The results reveal a strong positive relationship ($p = 0.002$) where an increase in inflow at Zhengyixia of 1×10^8 m^3 will increase the fractional area of irrigation by around 0.1 %.

The results allow us to modify earlier expression by replacing dA_I^* with $\alpha\, dR$ (Fig. 8) and df_D with $\beta\, dP$ (Fig. 7), respectively,

$$\frac{df_V}{f_V} \sim \frac{f_I}{f_V}\alpha\, dR + \frac{A_D^*}{f_V}\beta\, dP. \quad (7)$$

Expressing that in a relative form we have

$$\frac{df_V}{f_V} \sim \frac{f_I}{f_V}\alpha\, R\frac{dR}{R} + \frac{A_D^*}{f_V}\beta\, P\frac{dP}{P}.$$

Taking the long-term mean annual values ($f_I = 0.17$, $f_V = 0.038$, $R = 9.67 \times 10^8$, $P = 47.5$, $A_D^* = 0.97$) and the empirical coefficients ($\alpha = 0.0011$, Fig. 8; $\beta = 0.00017$, Fig. 7) we have

$$\frac{df_V}{f_V} \sim 0.05\frac{dR}{R} + 0.21\frac{dP}{P} = X_R + X_P. \quad (8)$$

The empirically based equation predicts that a 1 % variation in runoff would lead to a 0.05 % variation in f_V while a 1 % variation in precipitation would increase f_V by 0.21 %. Finally, we use the runoff and precipitation data to estimate the relative changes in regional vegetation cover. The overall results show that the model developed here accounts for ca. 52 % of the total variance in regional vegetation cover (Fig. 9). It varied from 45 to 62 % depending on different precipitation databases (Fig. S4 in the Supplement.).

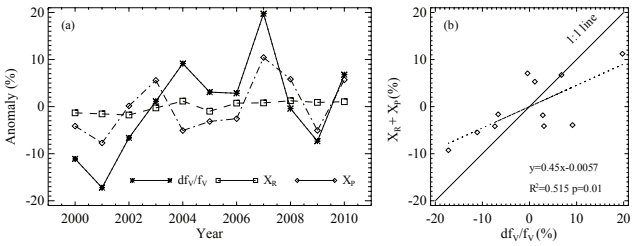

Figure 9. Relationship between regional vegetation cover and water availability. Relative variations **(a)**, and the observed annual changes in relative vegetation cover ($\mathrm{d}f_V/f_V$) versus predicted changes from water availability of runoff (X_R) and precipitation (X_P) **(b)**.

4 Discussion

In this study, we focused on a hyper-arid oasis–desert system where agricultural crops (artificial oasis) and groundwater-fed native vegetation (natural oasis) that occupy some 4 % of the entire region are concentrated along the Heihe River. As is well known, it is very hard to evaluate sparse desert vegetation cover in hyper-arid regions at a regional scale owing to coarse spatial and spectral resolution (Fensholt and Proud, 2012). However, the MODIS sensor has spectral bands that are specifically designed for vegetation monitoring and MODIS-based vegetation indices are known to perform well in discriminating vegetation differences in both sparsely and densely vegetated areas (Huete et al., 2002). Therefore, a vegetation index from MODIS with 250 m spatial resolution is likely to be appropriate for monitoring of fragmented landscapes of drylands, e.g. Central Asia (Dubovyk et al., 2013) and provides a potentially useful data source to evaluate regional vegetation change.

We found it necessary to restrict our analysis to the growing season to avoid noise apparently caused by snow and ice. With that pre-processing, our results showed that the mean growing season fractional vegetation cover (f_V) in Ejina showed a steady increase from $\sim$3.2 % in 2000 and rising to $\sim$4.5 % in 2012. The key question is what caused this change: the general climate variability or human-induced land use changes relating to irrigation?

We were able to identify the crops and green native vegetation along the river using the elevated NDVI signal during the April–October growing season, but we were unable to separate the crops from the native vegetation using the MODIS NDVI satellite data. Therefore, the entire region was split into two land cover types, denoted here as desert and irrigation oasis (that includes native vegetation along the river) for each year. Desert is distinguished from irrigated lands using a simple maximal NDVI threshold (Fig. 3).

Regional vegetation cover depends on both the desert and irrigated vegetation cover and their area fractions. Regional vegetation cover in the downstream of the Heihe River basin (2000–2012) is highly sensitive to variations in the area of irrigated land (Eq. 5). Over the whole period we found that the contributions to regional vegetation cover change due to changes in irrigated vegetation cover (f_I) and the area fraction (A_I^*) were 7.8 and 20.5 %, respectively, while changes in the non-irrigated vegetation cover (f_D) and area fraction (A_D^*) accounted for 75.8 %, and -4.1 %, respectively. Uncertainty analysis indicated that the fractional changes were not especially sensitive to the assumed NDVI threshold that was used to delineate desert from irrigated lands (Table 1). With that, our final result was that the relative vegetation change over the basin was most sensitive to changes in greenness of desert vegetation ($\sim$75 %, Table 1) and in the area of irrigation ($\sim$21 %, Table 1). The remaining terms (greenness of irrigated vegetation, area of desert) could be ignored.

To be able to prognostically estimate changes in relative vegetation cover, we sought an empirical relationship between desert greenness and precipitation (Fig. 7) and between the extent of irrigation and runoff in the previous year (Fig. 8). Gridded databases supplied a useful way to estimate the precipitation and its spatial distribution. Therefore, as expected, vegetation cover in the non-irrigated desert region (f_D) was strongly related to annual precipitation (Fig. 7) (Bhuiyan, 2008; D'Odorico and Porporato, 2006). The underlying basis of the aforementioned runoff–irrigation area relationship would be complex and would involve a lag because (i) farmers may anticipate future planting areas based on runoff from the previous years and (ii) the runoff recharges the local groundwater that is subsequently used by the local population (for irrigation) and by the native oasis vegetation. The lagged relationship between runoff and the area of irrigation may provide a useful empirical basis for forecasting and confirms the importance of managing human impact to achieve targeted improvements in the regional ecology.

It is difficult to discriminate between the effects of climate change and of human activities on regional vegetation change in arid regions (Zhou et al., 2013). In northwest China, previous work has suggested that precipitation is the most important factor (Ma and Frank, 2006) while other studies concluded that climate factors only played a small role, with the major cause of regional vegetation change being caused by agricultural activities (Kong et al., 2010; Zhou et al., 2013). Previous studies trying to separate the change into climate versus human causes have been limited to either qualitative distinctions (Dai et al., 2011), model estimation (C. X. Zhang et al., 2011; Zhou et al., 2013), and regression and residual approximation (Wang et al., 2012). To resolve those differences, we used a formal analytic framework to attribute the change of regional vegetation cover between climatic and human drivers.

The reason why we can use this method in this ecologically delicate and highly important area is that most human activities are focused around the irrigated oases that account for 3–5 % of the total area. This is typical of oasis–desert landscapes which dominate Central Asia, with widespread

irrigation oases. In this system, the allocation of water resources is critical in achieving a balance among different oases as well as between human water appropriation for irrigation and ecological conservation. The overuse of water in the upper and middle reaches associated with increased irrigation made significant reductions in river flows to the downstream oases and accelerated desertification. A similar overuse of water for irrigation also happened in the Aral Sea. The water withdrawal for agricultural expansion (e.g. from about 4.5 Mha in 1960 to almost 7.9 Mha by 1999) led to a dramatic shrinkage of the Aral Sea that has attracted the attention of the international scientific community over the last few decades (Micklin, 1988; Whish-Wilson, 2002; Lioubimtseva et al., 2005). In the last few decades, runoff from mountains has shown a positive trend, with more precipitation and warmer climate (Unger-Shayesteh et al., 2013; Wang et al., 2013a). However, rational distribution and sustainable management of water resources is still a long-term and arduous task. Our results suggest that it is possible to use remotely sensed data to provide practical support in assessing the ecological status of irrigation regions that surround most Central Asian rivers.

5 Conclusions

We found that the regional fractional vegetation cover f_V in the downstream parts of the greater Heihe River basin increased by 25 % from 2000 to 2012. The largest contribution was due to a slight greening of the desert regions that was consistent with increased precipitation over the period. The other main contribution to the regional trend was an expansion of irrigated areas (including native vegetation dependent on groundwater) along the Heihe River that was found to be dependent on the runoff in the previous year. In conclusion, water availability both from precipitation and runoff can explain around 52 % of the total variance in regional vegetation cover over the period in this extremely arid environment. This study showed that it is feasible to separate the variations in regional vegetation cover that are due to changes in the climate from those due to changes in human activities given an appropriate regional context.

The Supplement related to this article is available online at doi:10.5194/hess-18-3499-2014-supplement.

Acknowledgements. This study was supported by the National Program on Key Basic Research Project of China (2010CB951003) and the China Scholarship Council. The vegetation type data set is provided by Environmental and Ecological Science Data Center for West China, National Natural Science Foundation of China (http://westdc.westgis.ac.cn). We thank three anonymous reviewers for their insightful comments and suggestions that improved this manuscript.

Edited by: P. Saco

References

Angelini, I. M., Garstang, M., Davis, R. E., Hayden, B., Fitzjarrald, D. R., Legates, D. R., Greco, S., Macko, S., and Connors, V.: On the coupling between vegetation and the atmosphere, Theor. Appl. Climatol., 105, 243–261, doi:10.1007/s00704-010-0377-5, 2011.

Bhuiyan, C.: Desert vegetation during droughts: response and sensitivity, The International Archives of the Photogrammetry, Remote Sens. Spatial Inform. Sci., 37, 907–912, 2008.

Bonan, G. B., Levis, S., Sitch, S., Vertenstein, M., and Oleson, K. W.: A dynamic global vegetation model for use with climate models: concepts and description of simulated vegetation dynamics, Global Change Biol., 9, 1543–1566, doi:10.1046/j.1365-2486.2003.00681.x, 2003.

Bond, W., Midgley, G., and Woodward, F.: The importance of low atmospheric CO_2 and fire in promoting the spread of grasslands and savannas, Global Change Biol., 9, 973–982, doi:10.1046/j.1365-2486.2003.00577.x, 2003.

Bounoua, L., Hall, F. G., Sellers, P. J., Kumar, A., Collatz, G. J., Tucker, C. J., and Imhoff, M. L.: Quantifying the negative feedback of vegetation to greenhouse warming: A modeling approach, Geophys. Res. Lett., 37, L23701, doi:10.1029/2010gl045338, 2010.

Box, E. O., Holben, B. N., and Kalb, V.: Accuracy of the Avhrr Vegetation Index as a Predictor of Biomass, Primary Productivity and Net CO_2 Flux, Veget., 80, 71–89, doi:10.1007/Bf00048034, 1989.

Carlson, T. N. and Ripley, D. A.: On the relation between NDVI, fractional vegetation cover, and leaf area index, Remote Sens. Environ., 62, 241–252, doi:10.1016/S0034-4257(97)00104-1, 1997.

Chen, J., Jonsson, P., Tamura, M., Gu, Z. H., Matsushita, B., and Eklundh, L.: A simple method for reconstructing a high-quality NDVI time-series data set based on the Savitzky-Golay filter, Remote Sens. Environ., 91, 332–344, doi:10.1016/j.rse.2004.03.014, 2004.

Chen, M. Y., Xie, P. P., Janowiak, J. E., and Arkin, P. A.: Global land precipitation: A 50-yr monthly analysis based on gauge observations, J. Hydrometeorol., 3, 249–266, doi:10.1175/1525-7541(2002)003<0249:Glpaym>2.0.Co;2, 2002.

Dai, S. P., Zhang, B., Wang, H. J., Wang, Y. M., Guo, L. X., Wang, X. M., and Li, D.: Vegetation cover change and the driving factors over northwest China, J. Arid Land, 3, 25–33, doi:10.3724/sp.j.1227.2011.00025, 2011.

Dirnböck, T., Grandin, U., Bernhardt-Römermann, M., Beudert, B., Canullo, R., Forsius, M., Grabner, M. T., Holmberg, M., Kleemola, S., and Lundin, L.: Forest floor vegetation response to nitrogen deposition in Europe, Global Change Biol., 20, 429–440, doi:10.1111/gcb.12440, 2014.

D'Odorico, P. and Porporato, A.: Dryland ecohydrology, Springer, 2006.

Donohue, R. J., McVicar, T. R., and Roderick, M. L.: Climate-related trends in Australian vegetation cover as inferred from satellite observations, 1981-2006, Global Change Biol., 15, 1025–1039, doi:10.1111/j.1365-2486.2008.01746.x, 2009.

Donohue, R. J., Roderick, M. L., McVicar, T. R., and Farquhar, G. D.: Impact of CO_2 fertilization on maximum foliage cover across the globe's warm, arid environments, Geophys. Res. Lett., 40, 3031–3035, doi:10.1002/grl.50563, 2013.

Dubovyk, O., Menz, G., Conrad, C., Kan, E., Machwitz, M., and Khamzina, A.: Spatio-temporal analyses of cropland degradation in the irrigated lowlands of Uzbekistan using remote-sensing and logistic regression modeling, Environ. Monit. Assess., 185, 4775–4790, doi:10.1007/s10661-012-2904-6, 2013.

Fang, J. Y., Piao, S. L., He, J. S., and Ma, W. H.: Increasing terrestrial vegetation activity in China, 1982–1999, Sci. China Ser. C, 47, 229–240, doi:10.1360/03yc0068, 2004.

Fensholt, R. and Proud, S. R.: Evaluation of earth observation based global long term vegetation trends – Comparing GIMMS and MODIS global NDVI time series, Remote Sens. Environ., 119, 131–147, doi:10.1016/j.rse.2011.12.015, 2012.

Fensholt, R., Rasmussen, K., Kaspersen, P., Huber, S., Horion, S., and Swinnen, E.: Assessing Land Degradation/Recovery in the African Sahel from Long-Term Earth Observation Based Primary Productivity and Precipitation Relationships, Remote Sens., 5, 664–686, doi:10.3390/Rs5020664, 2013.

Fu, K., Chen, X. P., Liu, Q. G., and Li, C. H.: Land use and land cover changes based on remote sensing and GIS in Heihe River basin, China, IEEE International Symposium on Geoscience and Remote Sensing, 23–28 July, Barcelona, 1790–1793, 2007.

Gerten, D., Schaphoff, S., Haberlandt, U., Lucht, W., and Sitch, S.: Terrestrial vegetation and water balance – hydrological evaluation of a dynamic global vegetation model, J. Hydrol., 286, 249–270, doi:10.1016/j.jhydrol.2003.09.029, 2004.

Goetz, S. J., Bunn, A. G., Fiske, G. J., and Houghton, R.: Satellite-observed photosynthetic trends across boreal North America associated with climate and fire disturbance, Proc. Natl. Acad. Sci. USA, 102, 13521–13525, doi:10.1073/pnas.0506179102, 2005.

Guo, Q. L., Feng, Q., and Li, J. L.: Environmental changes after ecological water conveyance in the lower reaches of Heihe River, northwest China, Environ. Geol., 58, 1387–1396, doi:10.1007/s00254-008-1641-1, 2009.

Harris, I., Jones, P., Osborn, T., and Lister, D.: Updated high-resolution grids of monthly climatic observations–the CRU TS3. 10 Dataset, Int. J. Climatol., 34, 623–642, doi:10.1002/joc.3711, 2013.

Herrmann, S. M., Anyamba, A., and Tucker, C. J.: Recent trends in vegetation dynamics in the African Sahel and their relationship to climate, Global Environ. Chang., 15, 394–404, doi:10.1016/j.gloenvcha.2005.08.004, 2005.

Huete, A., Didan, K., Miura, T., Rodriguez, E. P., Gao, X., and Ferreira, L. G.: Overview of the radiometric and biophysical performance of the MODIS vegetation indices, Remote Sens. Environ., 83, 195–213, doi:10.1016/S0034-4257(02)00096-2, 2002.

Hutchinson, C. F., Unruh, J. D., and Bahre, C. J.: Land use vs. climate as causes of vegetation change: a study in SE Arizona, Global Environ. Chang., 10, 47–55, doi:10.1016/S0959-3780(00)00009-1, 2000.

Jia, L., Shang, H., Hu, G., and Menenti, M.: Phenological response of vegetation to upstream river flow in the Heihe Rive basin by time series analysis of MODIS data, Hydrol. Earth. Syst. Sci., 15, 1047–1064, doi:10.5194/hess-15-1047-2011, 2011.

Jin, X. M., Schaepman, M., Clevers, J., Su, Z. B., and Hu, G. C.: Correlation Between Annual Runoff in the Heihe River to the Vegetation Cover in the Ejina Oasis (China), Arid Land Res. Manag., 24, 31–41, doi:10.1080/15324980903439297, 2010.

Kong, W., Sun, O., Chen, Y., Yu, Y., and Tian, Z.: Patch-level based vegetation change and environmental drivers in Tarim River drainage area of West China, Landscape Ecol., 25, 1447–1455, doi:10.1007/s10980-010-9505-y, 2010.

Lim, C., Kafatos, M., and Megonigal, P.: Correlation between atmospheric CO_2 concentration and vegetation greenness in North America: CO_2 fertilization effect, Climate Res., 28, 11–22, doi:10.3354/cr028011, 2004.

Lioubimtseva, E. and Henebry, G. M.: Climate and environmental change in arid Central Asia: Impacts, vulnerability, and adaptations, J. Arid Environ., 73, 963–977, doi:10.1016/j.jaridenv.2009.04.022, 2009.

Lioubimtseva, E., Cole, R., Adams, J. M., and Kapustin, G.: Impacts of climate and land-cover changes in arid lands of Central Asia, J. Arid Environ., 62, 285–308, doi:10.1016/j.jaridenv.2004.11.005, 2005.

Ma, M. and Frank, V.: Interannual variability of vegetation cover in the Chinese Heihe River Basin and its relation to meteorological parameters, Int. J. Remote Sens., 27, 3473–3486, doi:10.1080/01431160600593031, 2006.

Micklin, P. P.: Desiccation of the Aral Sea – a Water Management Disaster in the Soviet-Union, Science, 241, 1170–1175, doi:10.1126/science.241.4870.1170, 1988.

Mohammat, A., Wang, X. H., Xu, X. T., Peng, L. Q., Yang, Y., Zhang, X. P., Myneni, R. B., and Piao, S. L.: Drought and spring cooling induced recent decrease in vegetation growth in Inner Asia, Agr. Forest. Meteorol., 178, 21–30, doi:10.1016/j.agrformet.2012.09.014, 2013.

Myneni, R. B., Keeling, C. D., Tucker, C. J., Asrar, G., and Nemani, R. R.: Increased plant growth in the northern high latitudes from 1981 to 1991, Nature, 386, 698–702, doi:10.1038/386698a0, 1997.

Nemani, R. R., Keeling, C. D., Hashimoto, H., Jolly, W. M., Piper, S. C., Tucker, C. J., Myneni, R. B., and Running, S. W.: Climate-driven increases in global terrestrial net primary production from 1982 to 1999, Science, 300, 1560–1563, doi:10.1126/science.1082750, 2003.

Pielke, R. A., Avissar, R., Raupach, M., Dolman, A. J., Zeng, X. B., and Denning, A. S.: Interactions between the atmosphere and terrestrial ecosystems: influence on weather and climate, Global Change Biol., 4, 461–475, doi:10.1046/j.1365-2486.1998.t01-1-00176.x, 1998.

Qin, D. J., Zhao, Z. F., Han, L. F., Qian, Y. P., Ou, L., Wu, Z. Q., and Wang, M. C.: Determination of groundwater recharge regime and flowpath in the Lower Heihe River basin in an arid area of Northwest China by using environmental tracers: Implications for vegetation degradation in the Ejina Oasis, Appl. Geochem., 27, 1133–1145, doi:10.1016/j.apgeochem.2012.02.031, 2012.

Rahimov, S.: Impacts of climate change on water resources in Central Asia, Documentos CIDOB. Asia, 33–56, 2009.

Schneider, U., Fuchs, T., Meyer-Christoffer, A., and Rudolf, B.: Global precipitation analysis products of the GPCC, Global Precipitation Climatology Centre (GPCC), DWD, Internet Publikation, 1–12, 2008.

Sun, F. B., Roderick, M. L., and Farquhar, G. D.: Changes in the variability of global land precipitation, Geophys Res. Lett., 39, L19402, doi:10.1029/2012gl053369, 2012.

Thonicke, K., Venevsky, S., Sitch, S., and Cramer, W.: The role of fire disturbance for global vegetation dynamics: coupling fire into a Dynamic Global Vegetation Model, Global Ecol. Biogeogr., 10, 661–677, 2001.

Tucker, C. J.: Red and Photographic Infrared Linear Combinations for Monitoring Vegetation, Remote Sens. Environ., 8, 127–150, doi:10.1016/0034-4257(79)90013-0, 1979.

Unger-Shayesteh, K., Vorogushyn, S., Farinotti, D., Gafurov, A., Duethmann, D., Mandychev, A., and Merz, B.: What do we know about past changes in the water cycle of Central Asian headwaters? A review, Global Planet. Change, Part A, 110, 4–25, doi:10.1016/j.gloplacha.2013.02.004, 2013.

Wang, P., Zhang, Y. C., Yu, J. J., Fu, G. B., and Ao, F.: Vegetation dynamics induced by groundwater fluctuations in the lower Heihe River Basin, northwestern China, J. Plant Ecol. UK, 4, 77–90, doi:10.1093/Jpe/Rtr002, 2011.

Wang, T., Sun, J. G., Han, H., and Yan, C. Z.: The relative role of climate change and human activities in the desertification process in Yulin region of northwest China, Environ. Monit. Assess., 184, 7165–7173, doi:10.1007/s10661-011-2488-6, 2012.

Wang, Y., Shen, Y., Chen, Y., and Guo, Y.: Vegetation dynamics and their response to hydroclimatic factors in the Tarim River Basin, China, Ecohydrology, 6, 927–936, doi:10.1002/eco.1255, 2013a.

Wang, Y., Feng, Q., Chen, L. J., and Yu, T. F.: Significance and Effect of Ecological Rehabilitation Project in Inland River Basins in Northwest China, Environ. Manage., 52, 209–220, doi:10.1007/s00267-013-0077-x, 2013b.

Whish-Wilson, P.: The Aral Sea environmental health crisis, Journal of Rural and Remote Environmental Health, 1, 29–34, 2002.

Yao, T. D., Wang, Y. Q., Liu, S. Y., Pu, J. C., Shen, Y. P., and Lu, A. X.: Recent glacial retreat in High Asia in China and its impact on water resource in Northwest China, Sci. China Ser. D, 47, 1065–1075, doi:10.1360/03yd0256, 2004.

Yu, J. and Wang, P.: Relationship between Water and Vegetation in the Ejina Delta, Bull. Chinese Acad. Sci., 26, 68–75, 2012.

Zhang, C. X., Wang, X. M., Li, J. C., and Hua, T.: Roles of climate changes and human interventions in land degradation: a case study by net primary productivity analysis in China's Shiyanghe Basin, Environ. Earth Sci., 64, 2183–2193, doi:10.1007/s12665-011-1046-4, 2011.

Zhang, Y. C., Yu, J. J., Wang, P., and Fu, G. B.: Vegetation responses to integrated water management in the Ejina basin, northwest China, Hydrol. Process., 25, 3448–3461, doi:10.1002/Hyp.8073, 2011.

Zhou, W., Sun, Z., Li, J., Gang, C., and Zhang, C.: Desertification dynamic and the relative roles of climate change and human activities in desertification in the Heihe River Basin based on NPP, J. Arid Land, 5, 465–479, doi:10.1007/s40333-013-0181-z, 2013.